Sensors & Transducers, Vol. 170, Issue 5, May 2014, pp. 274-280

www.sensorsportal.com

Sensors & Transducers

http://www.sensorsportal.com

A Super-resolution Algorithm Based on SURF and POCS for 3D Bionics PTZ

Hengyu LI, Jiqing CHEN, Shaorong XIE and Jun LUO
School of Mechatronics Engineering and Automation, Shanghai University,
149 Yanchang Road, Zhabei District, Shanghai, 200072, China
Tel.: 86+21+56334839
E-mail: lihengyu@shu.edu.cn

Received: 30 March 2014 /Accepted: 30 April 2014 /Published: 31 May 2014

Abstract: Image super-resolution algorithm improves image resolution in software. Before image tracking, it needs to enhance image resolution to improve the image tracking accuracy of the bionic eye. The traditional super-resolution reconstruction method can't satisfy the accuracy and real-time system, so this paper proposes super-resolution image reconstruction algorithm based on SURF (Speeded up Robust Features) and POCS (Projections Onto Convex Sets). The algorithm applies SURF algorithm on image registration and uses RANSAC (RANdom SAmple Consensus) algorithm to kick out fault feature to improve the accuracy of image registration. After motion estimation, this paper applies POCS algorithm to reconstruct a super-resolution image. Finally, some experiments are performed on the platform of a bionic eye, which show that the algorithm can better improve the image resolution and reach real-time requirements to some extent, and providing basis for the subsequent image tracking. *Copyright © 2014 IFSA Publishing, S. L.*

Keywords: Super-resolution Algorithm, SURF, POCS, Bionics PTZ, RANdom SAmple Consensus.

1. Introduction

Vision technology gets more attention in the study of robot technology. It is appropriate to conduct image tracking for robots because human eye can track fast moving objects. Image resolution has a certain effect on the image tracking accuracy. There are two common methods to improve image resolution, which is improving the resolution of the camera or using some super-resolution algorithms. For better portability, this paper chooses the algorithm to improve the image resolution. Image super-resolution reconstruction is to reconstruct a high-resolution image by complementary information of multiple low-resolution images, the core idea of which is to exchange time bandwidth for a high-resolution image.

Super-resolution image reconstruction algorithm can be divided into spatial method and frequency domain method [1]. Frequency domain method is intuitive but it is limited in linear space unchanged and it contains only a limited spatial prior knowledge by using the global translational motion degradation model. Spatial domain is modeling of spatial domain factors which affecting the low-resolution images results. Therefore the spatial domain method is closer to the actual application.

In previous researches, the maximum a posterior (MAP) method [2-3], the projection on convex sets (POCS) method [4-5], the iterative back projection method [6-7], and the wavelet-based method [8] are extensively studied. These algorithms improve resolution to some extent, but there are still some sub-pixel errors.

Article number P_2072

In recent years, SIFT (Scale Invariant Feature Transform) algorithm [9] is introduced to the super resolution reconstruction. Seong Y. M. et al proposed a super-resolution reconstruction method [10] of low-resolution images sequence, which applied the SIFT algorithm in image registration firstly and then get high-resolution images by the learning super-resolution algorithm. Compared to the previous methods, SIFT have some improvement for super-resolution accuracy, but is time-consuming. It cannot satisfy real-time requirements.

Since the above algorithm can't satisfy the accuracy and real-time requirements simultaneously. As the precision and speed of SURF algorithms is better than that of SIFT algorithm, this paper proposes a super-resolution algorithm based on SURF [11-13] and POCS. Experimental results show that the algorithm can satisfy the accuracy and real-time requirements. The algorithm is shown in Fig. 1. This paper is organized as follows: Part II describes the design of bionic eye motion platform; Part III describes the model of super-resolution reconstruction; Part IV introduces the image registration algorithm based SURF; Part V describes the principle and process of POCS algorithm; part VI mainly describes experiments and experiments show that the algorithm can satisfy the requirements of accuracy and real-time for the system.

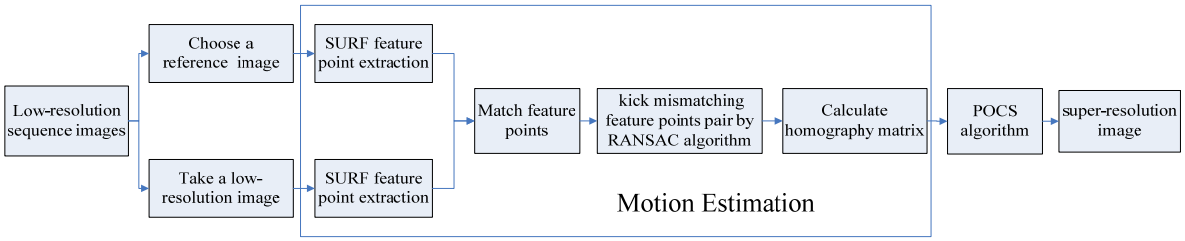

Fig. 1. The process of the algorithm based on SURF and POCS.

2. The Design of 3D Bionics PTZ

Currently the majority of robots on the market are only equipped with 2D bionics eye movement platform, which is different from the human eye movement. The human eye has 3 rotational degrees of freedom, so this paper designs a spherical parallel mechanism according to human eye movement characteristics and structure. The system has a spin degree of freedom that previous robot eyeballs system don't have, thus improving the image quality by robot's stance or the change targets posture, reducing the difficulty and complexity of the human eye observing and computer image processing.

The spherical parallel mechanism designed in this paper is shown as Fig. 2(a), which is consisted of a top platform (eye), a bottom platform, 3 pair branches which consisted with down links and up links. The motor fixed in bottom platform. Motor and down links, down links and up links, eyeballs and up links are connected by revolute pair. 9 revolute axes intersect at point O, called the center of mechanism rotation. Any point on the links of the mechanism is constrained by the rotational center. Relative movements between the links are rotational around the respective axis which penetrates the rotation center, so the moving platform has 3 rotational degrees of freedom relative to the stationary platform. The eye can realize 3 rotation degrees of freedom relative to the base by 3 motors. Fig. 2(b) is a 3D modeling of bionic platform designed in this paper and Fig. 2(c) is the object.

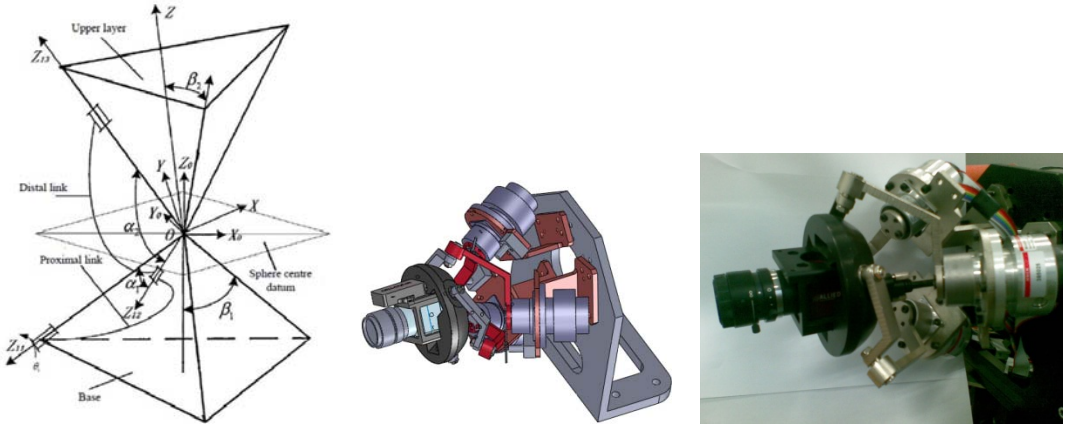

(a) (b) (c)

Fig. 2. Structure design of 3D bionic PZT.

3. The Model of Super-resolution Reconstruction

3.1. Degradation Model

Firstly introduction a common image observation model [15]. Observation model is generated after a series of ideal image degradation. The factors affect image degradation including atmospheric disturbances, the difference of the optical system, blur generated by movement, noise and down sampling, etc. All of these factors make image distortion and blur. The degradation processes shows as Fig. 3.

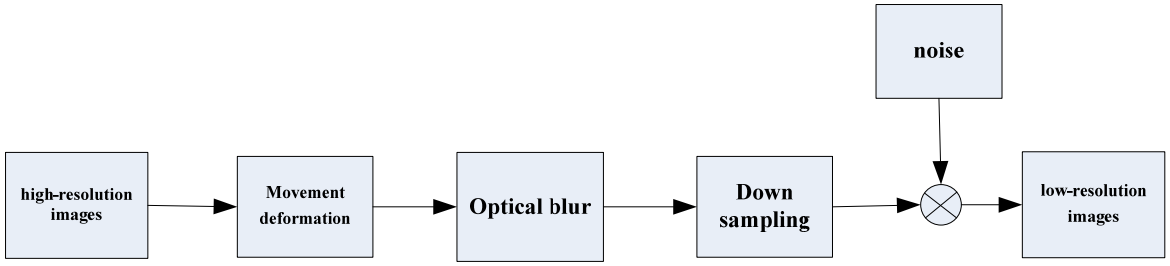

Fig. 3. The processes of image degradation.

If X is the ideal image, Y_i is sequence of low-resolution images obtained by observation, image forming process can be expressed as:

$$Y_i = MHFX + n_i \qquad i = 1,2,...,k\,, \tag{1}$$

where i is the number of frame, k is the low-resolution image frames, Y is the LNx1Column vectors, represents low-resolution images, X is the $qLqN$x1 Column vectors, represents high-resolution images, q is the amplification coefficient, M is the $qLqN$x $qLqN$ down sampling matrix, n_i is the image noise signal.

3.2. The Principles of Super-resolution Reconstruction

For a linear space invariant imaging system, the spatial domain imaging process can be described by the formula (2):

$$g(x) = h(x) * f(x)\,, \tag{2}$$

where $g(x)$ represents an image; $f(x)$ represents an objective; $h(x)$ represents point spread function; * denotes the convolution operation.

Realize super-resolution reconstruction is mainly based on the theory as follow [14-20]:

(1) Analytical continuation theory: if a function $f(x)$ is the airspace bounded, then the spectrum $F(u)$ is an analytic function. For analytic functions, it will be known anywhere if it confirm at a certain finite interval.

(2) Information superposition theory: the actual images have a non-negative and boundedness constraints for common imaging. That is the minimum light intensity of the target or image should be greater than 0, and it should have a certain size.

That can be represented by the following formula:

$$\begin{cases} f(x) > 0, x \in X \\ f(x) = 0, x \notin X \end{cases}, \tag{3}$$

where X means the size of the target.

(3) Nonlinear operation: considering the effect by the noise generated during imaging process, the general imaging process can be expressed as follows:

$$g(x) = h(x) * f(x) + n(x)\,, \tag{4}$$

where $n(x)$ represents the noise.

The flow of image super-resolution reconstruction is shown as Fig. 4. The purpose of image registration is getting the offset between low-resolution images. Then project the image to high-resolution grid and it needs to conduct interpolation directly or iterative interpolation to generate high-resolution images.

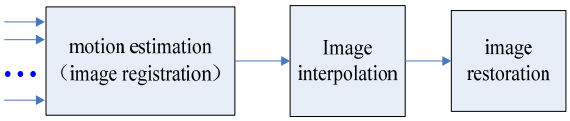

Fig. 4 The flow of image super-resolution reconstruction.

4. Image Registration Algorithm Based SURF

The SURF feature points have invariant size and direction, which extract by Herbert Bay, Tinne Tuytelaars and Luc Van Gool. Compared to SURF and SIFT, the SURF is higher accuracy and real-time. The processes of image registration algorithm show as Fig. 5.

Fig. 5. The processes of image registration algorithm.

4.1. SURF Feature Point Extraction

SURF feature points are extracted referencing to the principle of SURF algorithm [11-13], the steps as follows:

1) Convert a gray image into an integral image;

2) Calculate interest point of the image by Hessian matrix. Calculate one image point's local Maximum value of Hessian matrix determinant at different scales. Any point in the image $X(x, y)$, the Hessian matrix in the scale σ is defined as:

$$H(X,\sigma)=\begin{bmatrix} L_{xx}(X,\sigma) & L_{xy}(X,\sigma) \\ L_{xy}(X,\sigma) & L_{yy}(X,\sigma) \end{bmatrix}, \quad (5)$$

where $L_{xx}(X, \sigma)$ represents convolution of Gaussian second-order partial derivatives in direction X; $L_{xy}(X, \sigma)$ and $L_{yy}(X, \sigma)$ have a similar meaning.

3) Construct scale space. Establish image pyramid by adopting increasing size of filter box template.

4) SURF feature points extraction. Define local maximum value as a feature point by comparing a filter point with 26 points which includes 8 pixels in the same scale, 9 points adjacent to upper scale and the other adjacent to down scale.

5) Determine the characteristic vectors. Finally 64-dimensional feature vector is obtained.

4.2. Feature Point Matching

The paper uses the Euclidean distance between two feature vectors as two feature points' similarity measure after SURF feature vectors are generated.

$$d(X,Y)=\sqrt{\sum_{i=1}^{N}(x_i-y_i)^2}, \quad (6)$$

where $d(X, Y)$ represents the Euclidean distance between the feature vectors; $X=(x_1, x_2, x_3, \ldots x_N)$ and $Y=(y_1, y_2, y_3, \ldots y_N)$ respectively represent any point of images X and Y; i represents the i sub-component of the vector description; x_i and y_i respectively represent the i sub-component of the vector description of images X and Y; N means dimension of the feature vector, which is 64 in this paper.

This paper firstly takes a point from the reference image and then finds the nearest and next nearest point from another image. If the ratio between the square of nearest distance and the next nearest distance is less than 75 % [15], we regard the point pair as feature point pair. After that, this paper applies RANSAC algorithm [16] to kick wrong matching feature point pair.

4.3. Calculating Homographic Matrix

The relationship between the two images may be represented by a planar perspective transformation matrix.

$$X_i = HX_j, \quad (7)$$

where X_i represents $(x_i, y_i, 1)^T$; X_j represents $(x_j, y_j, 1)^T$; (x_i, y_i) and (x_j, y_j) are pairs of matching feature points; if matrix is a full rank of 3×3 matrix, it can be expressed as:

$$H=\begin{bmatrix} h_{11} & h_{12} & h_{13} \\ h_{21} & h_{22} & h_{23} \\ h_{31} & h_{32} & h_{33} \end{bmatrix}$$

5. Equations

5.1. The Principle of POCS Algorithm

POCS is an iterative process [4-5]: for the input image initial value, project it onto a convex set and iterate until it meets the requirement of the iteration. The solution of the intersection is considered to be the ideal image. The process of projection iteration is shown as formula:

$$f^{n+1}=P_N P_{N-1}\ldots P_1 f^n, \quad n=1,2,\ldots,N, \quad (8)$$

where f is the ideal high-resolution image; f^1 refer to the initial input value of iteration (the initial estimate of the high-resolution image); P_k is the projection operator of convex sets.

In the POCS algorithm, low-resolution image can be represented by mathematical model of high-resolution image.

$$g_l(m_1,m_2)=\sum_{(n_1,n_2)} f(n_1,n_2)h_l(m_1,m_2;n_1,n_2)+\eta_l(m_1,m_2), \quad (9)$$

where $g_l(m_1, m_2)$ means the l low-resolution image; $f(n_1, n_2)$ means high-resolution image; $h_l(m_1, m_2; n_1, n_2)$ means the function of PSF; $\eta(m_1, m_2)$ represents Gaussian noise.

Furthermore, it should satisfy the convex set data consistency and gray value limitation constraints.

Data consistency reflects the relationship between the pixels of high and low resolution images. The convex set is represented by (10):

$$C_{m_1,m_2,l}=\left\{f(m_1,m_2,k):|r^{(f)}(m_1,m_2,l)\le\delta_0(m_1,m_2,l)|\right\}, \quad (10)$$

$$r^{(f)}(m_1,m_2,l)=g(m_1,m_2,l) - \sum_{m_1,m_2} f(n_1,n_2,k)\bullet h(m_1,m_2;n_1,n_2,l)', \quad (11)$$

where $r^{(f)}(m_1, m_2, l)$ is the residual error of points in the convex sets; $\delta_0(m_1, m_2, l)$ is the statistical properties of Gaussian noise.

In fact, gray value limitation can be expressed as amplitude boundedness, and its mathematical expression is as follows:

$$C_A = \{f(x,y) \mid \alpha \le f(x,y) \le \beta\}, \quad (12)$$

where α=0; and β=255.

5.2. The Flow of POCS Algorithm

1) Conduct non-uniform interpolation for the reference image that is selected from low-resolution sequence images and the result of interpolation is considered as initial high-resolution image estimation $f^1(n_1, n_2, k)$.

2) Determine the *PSF* function of the model, that is $h_l(m_1, m_2; n_1, n_2)$, which is shown as formula (9).

3) Choose an image from low-resolution sequence images $g_l(m_1, m_2, l)$. If this image is the last image, the iteration stops.

4) Conduct image correction according to formula (9) for all pixels.

5) Convert to step 3.

6) Consider the obtained estimated image $f^1(n_1, n_2, k)$.as the required high-resolution image.

7) Constrain the magnitude by equation (12).

The algorithm flow chart is shown in Fig. 6.

6. Experimental Results and Analysis

The experiment was taken on the bionic eye platform. The system can control camera's displacement and rotation by controlling PTZ. The experiment reconstructs super-resolution based on four images. In order to facilitate better analysis on the effect of the algorithm, this paper designs 3 experiments, which are only rotation, only translation and both rotation and translation.

Fig. 7(a), (b), (c), (d) are four original low-resolution images that only translations, among which (a) is regarded as the reference image. Fig. 7(e) explain the 4 figures have enough feature point pairs, which is the registration result of (a) and (b), (a) and (c), (a) and (d). Fig. 7 (f) is super-resolution image obtained by the algorithm proposed in this paper. To better to illustrate the algorithm for the improving resolution, the wings in figure (a) and (f) are enlarged to the same size, which is shown as red circle in figure (a) and (f). Compare the red circle of the figure (a) and (f), especially the red box 1 and 2, red box portion in (f) is clear while that in (a) obvious mosaic. The experiment shows that the algorithm can perform well for low-resolution images that only translation.

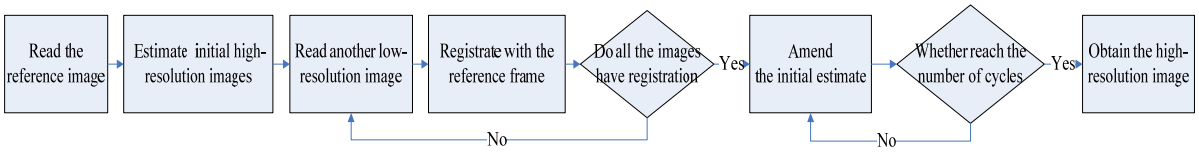

Fig. 6. The flow chart of POCS algorithm.

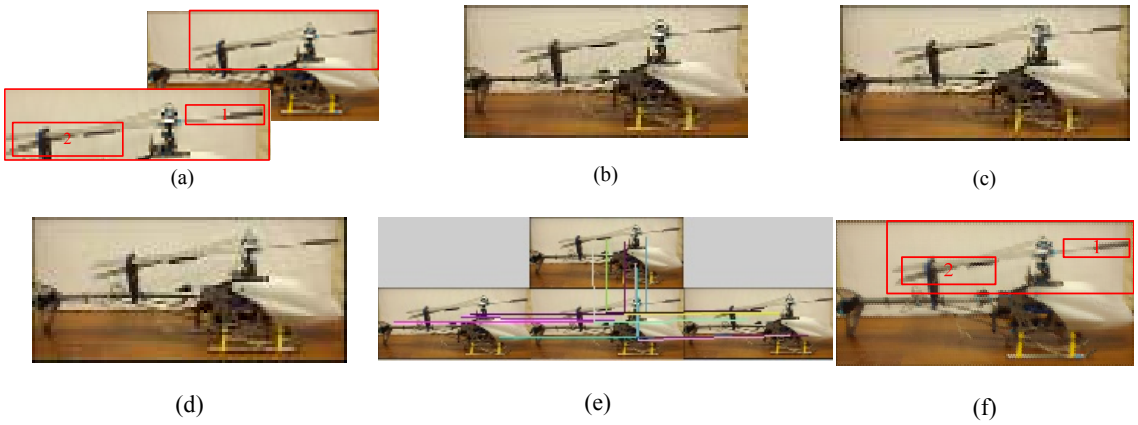

Fig. 7. The experimental result for low-resolution images that only translations ((a), (b), (c), (d) are original images, (e) the result of the matching feature points, (f) the super-resolution image).

Fig. 8(a), (b), (c), (d) are four original low-resolution images that only rotations, among which (a) is regarded as the reference image. Fig. 8(e) that can explain the 4 figures have enough feature point pairs is the registration result of (a) and (b), (a) and (c), (a) and (d). Fig. 8(f) is super-resolution image obtained by the algorithm proposed in this paper. To better to illustrate the algorithm for the improving resolution, red circle 1 and 2 in figure (a) are enlarged. Compare the bigger red circle 1 and 2 of the figure (a) and that in figure (f), the red circle in (f) is clear while that in (a) obvious mosaic. The experiment shows that the algorithm can perform well for low-resolution images that only rotation.

Fig. 9(a), (b), (c), (d) are four original low-resolution images that translations and rotations, among which (a) is regarded as the reference image. Fig. 9(e) can explain the 4 figures have enough feature point pairs and figure (f) is super-resolution image. To illustrate the algorithm effect, red small box 1 in figure (a) and (f) are enlarged to red big box, which are in the same level. The red big box in figure (a) has a clear gap in texture section while that in (f) is clear. The experiment shows that the algorithm can perform well for low-resolution images that translations and rotations.

SURF is 62-dimensional vector while SIFT is 128-dimensional vector, which greatly reduces the dimension of its operation in speed. The algorithm can handle about 20 images in 1s by super-resolution algorithm, and satisfy the real-time requirements of the system.

(a) (b) (c) (d) (e) (f)

Fig. 8. The experimental result for low-resolution images that only rotation ((a), (b), (c), (d) are original images, (e) the result of the matching feature points, (f) the super-resolution image).

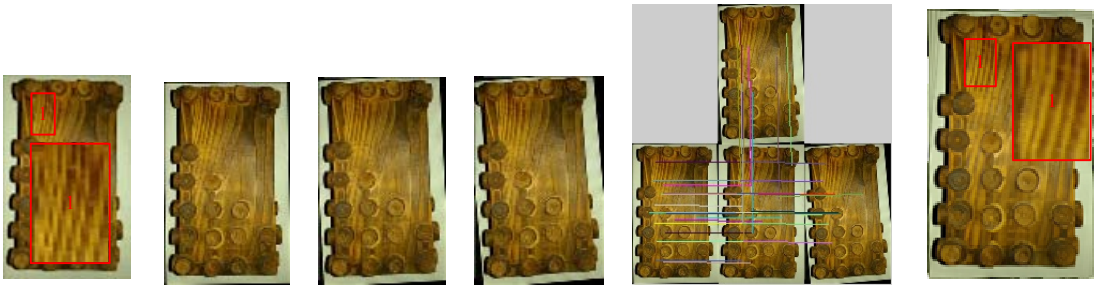

(a) (b) (c) (d) (e) (f)

Fig. 9. The experimental result for low-resolution images that translations and rotations ((a), (b), (c), (d) are original images, (e) the result of the matching feature points, (f) the super-resolution image).

7. Conclusions

To improve the accuracy of real-time tracking bionic eye, the system proposed a super-resolution reconstruction algorithm based on SURF and POCS based on the platform of bionic eye movement. This paper applies SURF algorithm for motion estimation that is image registration, and then adopts RANSAC algorithm to kick out false SURF feature points. After getting related motion estimation, the paper applies super-resolution reconstruction algorithm based on POCS. Finally, this paper performs experiments on the platform of a bionic eye, which shows that the algorithm can improve image resolution well and reach real-time requirements to some extent.

Acknowledgements

This project is supported by the National Nature Science Foundation of China (No.61375093), the outstanding academic leaders' plan of Shanghai (No.12XD1402600), and Shanghai Rising-Star Tracking Program (12QH1400900).

References

[1]. Chunxia Wang, Review of super-resolution image reconstruction techniques, *Computer Technology and Development*, Vol. 21, Issue 5, 2011, pp. 124-127.

[2]. G. Chantas, N. Galatsanos and N. Woods, Super-resolution based on fast registration and maximum a posteriori reconstruction, *IEEE Trans. Image Process.*, Vol. 16, Issue 7, 2007, pp. 1821–1830.

[3]. S. Farsiu, M. Robinson, M. Elad, and P. Milanfar, Fast and robust multiframe super-resolution, *IEEE Trans. Image Process.*, Vol. 13, Issue 10, 2004, pp. 1327–1344.

[4]. A. Patti, M. Sezan and A. Murat Tekalp, Super-resolution video reconstruction with arbitrary sampling lattices and nonzero aperture time, *IEEE Trans. Image Process.*, Vol. 6, Issue 8, 1997, pp. 1064–1076.

[5]. C. Fan, J. Zhu, J. Gong, and C. Kuang, Pocs super-resolution sequence image reconstruction based on improvement approach of keren registration method, *in Proceedings of the 6th Int. Conf. ISDA*, 2006, pp. 333–337.

[6]. M. Irani and S. Peleg, Motion analysis for image enhancement: Resolution, occlusion, and transparency, *Journal of Visual Communication and Image Representation*, Vol. 4 Issue 4, 1993, pp. 324–335.

[7]. A. Tekalp, M. Ozkan and M. Sezan, High-resolution image reconstruction from lower-resolution image sequences and space-varying image restoration, in *IEEE International Conference on Acoustics, Speech, and Signal Processing*, 1992, pp. 169–172.

[8]. H. Ji and C. Fermuller, Robust wavelet-based super-resolution reconstruction: Theory and algorithm, *IEEE Transactions on Pattern Analysis and Machine Intelligence*, Vol. 31, Issue 4, 2009, pp. 649–660.

[9]. D. G. Lowe, Distinctive image features from scale-invariant key points, *International Journal of Computer Vision*, Vol. 60, 2004, pp. 91-110.

[10]. Y. M. Seong, H. Park, A high-resolution image reconstruction method from low-resolution image sequence, in *Proceedings of the IEEE International Conference on Acoustics, Speech, and Signal Processing*, 1992, pp. 169-172.

[11]. H. Bay, T. Tuytelaars, and L. Van Gool, Surf: Speeded up robust features, *Computer Vision–ECCV*, 2006, pp. 404-417.

[12]. H. Bay, A. Ess, T. Tuytelaars, and L. Van Gool Speeded-up robust features (SURF). *Computer Vision and Image Understanding*, Vol. 110, 2008, pp. 346-359.

[13]. E. Yong, Investigation of mosaicing techniques for forward looking sonar, Master's thesis, *Heriot-Watt University,* 2011.

[14]. Yajing Zhang, Super-resolution algorithm for the reconstruction of the sequence of images, Master's thesis, *Northeastern University*, 2011.

[15]. B. Zitova and J. Flusser, Image registration methods: a survey, *Image and Vision Computing*, Vol. 21, 2003, pp. 977-1000.

[16]. M. A. Fischler and R. C. Bolles, Random sample consensus: a paradigm for model fitting with applications to image analysis and automated cartography, *Communications of the ACM,* Vol. 24, 1981, pp. 381-395.

[17]. X. Gao, K. Zhang, D. Tao and X. Li, Joint learning for single-image super-resolution via a coupled constraint, *IEEE Transactions on Image Processing,* Vol. 21, Issue 2, 2012, pp. 469-480.

[18]. X. Gao, K. Zhang, D. Tao and X. Li, Image super-resolution with sparse neighbor embedding, *IEEE Transactions on Image Processing,* Vol. 21, Issue 7, 2012, pp. 3194-3205.

[19]. K. Zhang, X. Gao, D. Tao and X. Li, Single image super-resolution with non-local means and steering kernel regression, *IEEE Transactions on Image Processing,* Vol. 21, Issue 11, 2012, pp. 4544-4556.

[20]. C. Kim, K. Choi and J. B. Ra, Example-Based Super-Resolution via Structure Analysis of Patches, *IEEE Signal Process. Lett.,* Vol. 20, Issue 4, 2013, pp. 407-410.
